

Dalton Transactions

Accepted Manuscript



This is an *Accepted Manuscript*, which has been through the Royal Society of Chemistry peer review process and has been accepted for publication.

Accepted Manuscripts are published online shortly after acceptance, before technical editing, formatting and proof reading. Using this free service, authors can make their results available to the community, in citable form, before we publish the edited article. We will replace this *Accepted Manuscript* with the edited and formatted *Advance Article* as soon as it is available.

You can find more information about *Accepted Manuscripts* in the [Information for Authors](#).

Please note that technical editing may introduce minor changes to the text and/or graphics, which may alter content. The journal's standard [Terms & Conditions](#) and the [Ethical guidelines](#) still apply. In no event shall the Royal Society of Chemistry be held responsible for any errors or omissions in this *Accepted Manuscript* or any consequences arising from the use of any information it contains.

Revised manuscript No. DT-ART-04-2015-001334

Dual mode signaling responses of a rhodamine based probe and on its immobilization onto silica gel surface for specific mercury ion detection

Ajoy Pal and Bamaprasad Bag*

Colloids and Materials Chemistry Department, Academy of Scientific and Innovative Research, CSIR-Institute of Minerals and Materials Technology, P.O.: R.R.L., Bhubaneswar-751 013, Odisha, India. Fax: (+) 91 674 258 1637; Tel: (+ 91) 674 237 9254, Email: bpbag@immt.res.in

Abstract

A 3-aminomethyl-(2-amino-1-pyridyl)- coupled amino-ethyl-rhodamine-B based probe (**2**) exhibited simultaneous chromogenic and fluorogenic dual mode signaling responses in presence of Hg(II) ion only among all metal ions investigated in organic aqueous medium. The spiro-cyclic rhodamine signaling subunit undergoes complexation induced structural transformation to result in absorption and fluorescence modulation. Its complexation induced signaling exhibited reversibility with various contrasting reagents having higher affinity towards Hg(II) ion, such as anions(AcO⁻) and competing chelating agents(En). It also exhibited Hg(II)-specific photophysical signaling responses when immobilized onto a silica gel surface attached through its amino-ethyl- receptor end, owing to its structure-conformational advantages for effective coordination. The surface modified silica appended with **2** (**SiR-1**), as evaluated through FTIR spectral pattern, thermogravimetric analysis, FESEM images and elemental analysis, X-ray diffraction, surface area determination and particle size analysis, also exhibited reversible Hg(II)-specific signaling in its suspension state in aqueous medium, enhancing the probe's utility for practical application such as detection, isolation and extraction of Hg(II) ion in presence of other competitive metal ions.

Introduction

Selective detection and quantification of heavy and transition metal ions is highly desirable when deviate from requisite concentration threshold in perspective of physiological health hazard and environmental impact assessment^{1,2}. Mercury induces such lethal toxic effects³ as it in its elemental and ionic forms potentially bio-transforms into methylmercury that subsequently bio-

accumulates through food-chain and enters into living functionalities to pose severe health hazards⁴. Most of methods currently followed for detection and monitoring of mercury ions involve sophisticated instrumentation and are either time consuming or inconvenient in terms of complicated sample preparation for such impact assessment. Among alternative feasible and viable approaches, chemosensory probes have proven⁵ to be promising owing to synthetic and operational advantages, selective and sensitive responses. Molecular ensembles with optical signaling module endorse highly selective and sensitive on-site, real-time detection of metal ions, where their design methodologies preferably include covalent architectures which execute both fluorogenic and chromogenic signaling in response to analyte binding. In this context, rhodamine based probes are advantageous owing to excellent spectroscopic features and contrast structure-function correlation of xanthene dyes. Despite of recent methodological advancements towards development of rhodamine based probes⁶ for metal ion detection, various issues pertaining to selectivity, sensitivity, reusability and real-time on-site operation are yet to be convincingly addressed and hence, promote for exploration into new probes with rhodamine signaling functionality for metal ion detection in general, contextually Hg(II) ion^{6g-o} detection.

Although effectiveness of such probes is more pronounced in homogeneous solution rendering advantages of real-time monitoring and paraphernalia of in-situ assessments, solid state chemosensors^{6l-o,7} in heterogeneous solid-liquid interfaces supplement more favorable features of spot-monitoring and explicit removal of targeted metal ion. Such materials can be repeatedly used with appropriate treatment, are useful in selective and efficient adsorbents for specific guest molecules in environmental pollutants, and can easily be isolated. One of the methodologies for development of such dual functional (chemosensor as well as adsorbent) material is immobilization of receptor segment of the probe containing coordination sites on to surface of a solid platform. Silica is one of the preferred⁸ matrixes as substrate in surface modified organic-inorganic hybrid because of its stable constitution through siloxane and silanol groups, tunable pore size, high specific surface area, a surface contained with high Si-OH functionality for further derivatization and easy recyclability. Considering advantages in signaling module with xanthene based dyes and silica matrix as solid substrate, few chemosensors^{6l-o,9-11} based on silica functionalized with rhodamine for detection of various metal ions are known in literature. Most of those silica-functionalized solid chemosensors for detection of Hg(II) ions execute their operation in mixed-organic aqueous medium, therefore, has implicated limitation in terms of

separation and extraction. Among promising ones, a recent report¹¹ on rhodamine-G based probe immobilized through carbohydrazide on to silica gel surface emphasized that longer carbon chain separating carbohydrazine group and imino-donor atom prevented chelation towards any metal ion, therefore failed to respond in complexation induced signaling in comparison to its shorter linker version which selectively sense and extract Hg(II) ion. Therefore, advantageous design are those which include (a) grafting of a prefabricated Hg(II)-specific rhodamine based probe onto silica surface and (b) availability of ample donor amino-groups for chelation and their appropriate spatial disposition for effective coordination is therefore anticipated to exhibit complexation induced dual mode signaling in response to the recognition process. We have demonstrated¹² earlier that suitable tuning of electron densities over donor amino groups through appropriate substitution and operational optimization of solvent medium induces selectivity in Hg(II)-specific dual mode signaling with derivatized ‘amino-ethyl-rhodamine’ based probes.

Aligned with the predetermined methodology for enhanced selectivity and sensitivity, we report herein dual mode ‘turn-on’ signaling responses of a ‘3-aminomethyl-(2-amino-1-pyridyl)’ functionalized amino-ethyl-rhodamine’ based probe **2** selectively in presence of Hg(II) ion and subsequent reversible ‘turn-off’ responses with various counter anions and/or chelating agents. Grafting of the Hg(II)-specific probe **2** onto silica surface through its ‘amino-ethyl-amino’ receptor lead to a surface modified chemosensor (**SiR-1**) which was also exhibited Hg(II)-specific fluorogenic and chromogenic signaling responses in aqueous medium. The selectivity in signaling, adsorption capability, and reversibility in complexation induced signals of surface modified silica gel appended with **2** endorsed its potential in selective detection and extraction of Hg(II) ions among coexisting competitive metal ions.

Experimental

Materials and methods

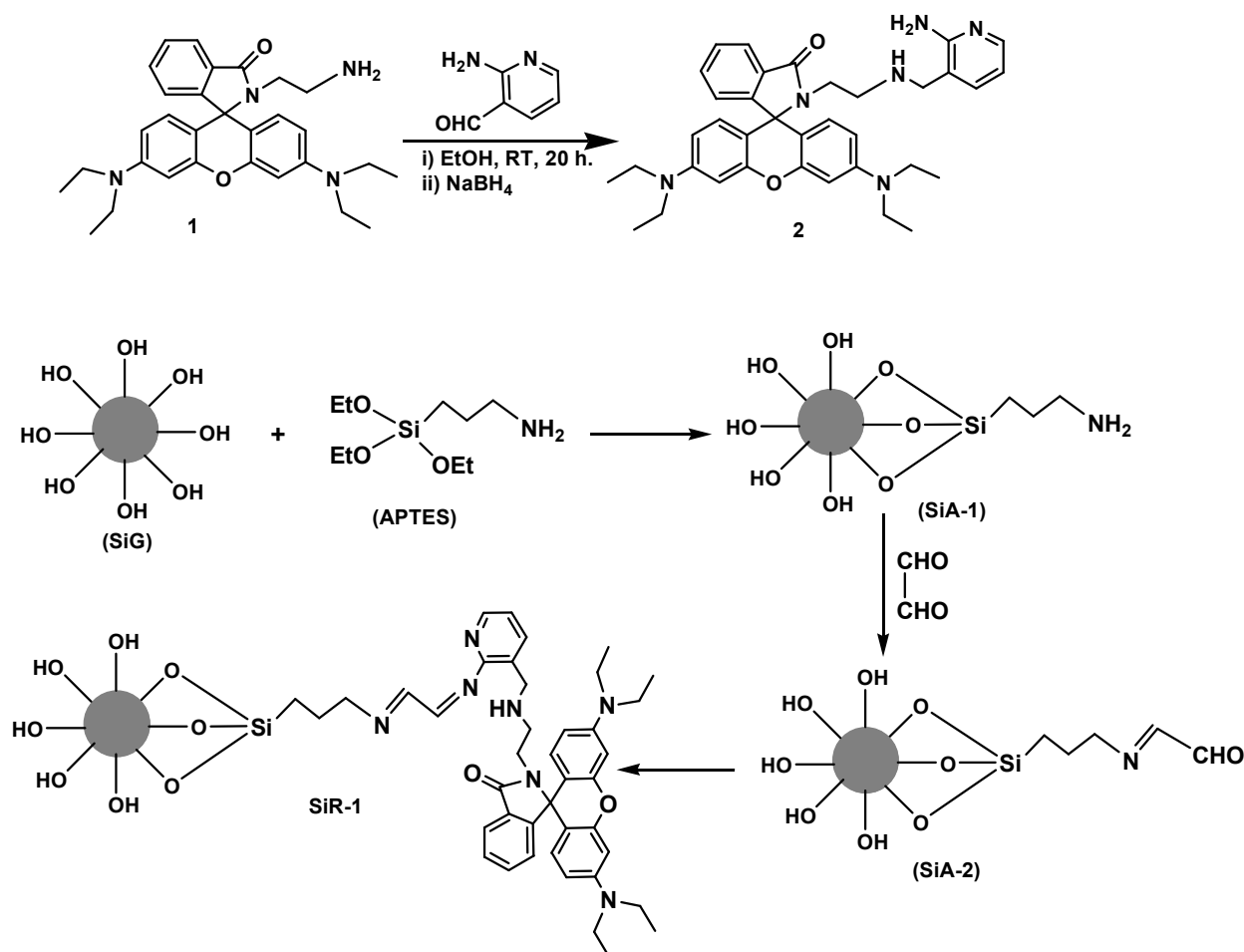
Unless otherwise mentioned, all the materials were used as received without further purification. Silica gel (60-120 mesh), glyoxal, 3-aminopropyl-triethoxy silane (APTES), and metal perchlorate salts were purchased from Sigma-Aldrich (India) Pvt. Ltd. Anhydrous sodium sulphate, acids, buffers and the solvents were received from S. D. Fine Chemicals (India). All solvents were freshly distilled prior to use in fluorescence measurements. Chromatographic separation was done by column chromatography using 100-200 mesh silica gel.

The compounds were characterized by elemental analyses, $^1\text{H-NMR}$, $^{13}\text{C-NMR}$ and mass (ESI) spectroscopy. $^1\text{H-NMR}$ and $^{13}\text{C-NMR}$ spectra were recorded on a JEOL JNM-AL400 FT V4.0 AL 400 (400 MHz and 100 MHz respectively) instrument in CDCl_3 with Me_4Si as the internal standard. Electrospray mass(ESI) spectral data were recorded on a MICROMASS QUATTRO II triple quadruple mass spectrometer. The dissolved samples of the compounds in suitable solvents were introduced into the ESI source through a syringe pump at the rate of $5\mu\text{L}/\text{min}$, ESI capillary was set at 3.5 kV with 40V cone voltage and the spectra were recorded at 6 s scans. Melting points were determined with a Stuart SMP20 melting point apparatus and were uncorrected. Elemental analyses were done in an Elementar Vario EL III Carlo Erba 1108 elemental analyzer. UV-visible spectra were recorded on a Perkin Elmer Lambda 650 UV/VIS spectrophotometer at 298 K in 10^{-4} - 10^{-5} M concentration. Steady-state fluorescence spectra were obtained with a Fluoromax 4P spectrofluorometer at 298 K. Single crystal X-ray data for **2** was collected at 100K on a Bruker KAPPA APEXII diffractometer. The powder X-ray diffraction patterns were obtained on a PANalytical XPERT-PRO diffractometer using Mo-K_α radiation operating at 40kV and 30mA. FT-IR spectra were recorded in a PerkinElmer Spectrum GX spectrometer. Thermo gravimetric analyses were done in METTLER TGA/SDTA 851^e instrument. Field Emission Scanning Electron Microscopic images and Energy Dispersive X-ray analysis were carried out in Supra 55 ZEISS (Germany) microscope equipped with 20 mm² OXFORD EDS detector. Atomic absorption spectroscopy for determining the unextracted mercury ions was measured by a Perkin Elmer AA 200 AAS spectrophotometer. The nitrogen adsorption isotherms were obtained at 77K in a Quantachrome autosorb-iQ automated gas-sorption analyzer and the BET surface area was calculated through ASiQwin software. The particle size distributions were obtained on a Malvern Mastersizer 2000 analyzer with water as dispersant. Fluorescence quantum yield of **2** alone and in presence of various metal ions was determined in each case by comparing the corrected spectrum with that of Rhodamine 6G in EtOH ¹³ by taking the area under total emission using the procedure reported¹⁴ in literature.

Synthesis and characterizations of compounds

Synthesis of Amino ethyl rhodamine, 1:

This compound was synthesized following the procedure reported¹⁵ earlier.



Scheme 1: Synthesis route to **2** and schematic representation of its immobilization onto silica gel surface.

Synthesis of probe 2

To a stirring ethanolic solution (15 mL) of **1** (0.485 g, 1 mmol), 2-amino pyridine-3-carboxaldehyde (0.124 g, 1 mmol) was added at a time and was allowed to stir for 20h. The Schiff base (imine) thus formed was reduced with NaBH₄ and was further refluxed for 1h to ensure completion of the reduction. The solvent was then evaporated to dryness under reduced pressure and water was added to the residual mass. The compound was extracted with CHCl₃ (3 × 30 mL). The combined organic layers were dried over anhydrous Na₂SO₄, filtered and evaporated under reduced pressure to obtain the desired product **2** as colorless compound. It was further purified by column chromatography using hexane and ethyl-acetate (3:7 v/v) mixture as eluent. The block-shaped, colourless single crystals suitable for X-ray diffraction were obtained

from ethyl acetate through slow-evaporation technique. Yield: 0.445 g (74.48%); mp: 112 °C; ESI-MS, m/z^+ (%): 591.25 [**2**]⁺ (33%); ¹H-NMR (400 MHz, CDCl₃, 25°C, TMS, δ): 7.819(m, J = 2.0 Hz, 2H), 7.372 (m, J = 3.2 Hz, 2H), 7.007 (t, J = 2.8 Hz, 2H), 6.423 (s, 1H), 6.405 (d, J = 2.0 Hz, 1H), 6.392 (s, 1H), 6.351 (s, 1H), 6.329 (s, 1H), 6.293 (d, J = 2.4 Hz, 2H), 6.18-6.151 (dd, J_1 = 6.4 Hz, J_2 = 2.4 Hz, 2H), 5.433 (s, 2H), 3.496 (s, 2H), 3.397-3.194 (m, 11H), 2.299 (t, J = 6.0 Hz, 2H), 1.283 (s, NH), 1.182 (s, NH), 1.103 (t, J = 7.2 Hz, 14H); ¹³C-NMR (100 MHz, CDCl₃, 25°C, TMS, δ): 168.87, 158.9, 153.51, 148.97, 146.55, 137.25, 132.65, 131.35, 128.87, 128.27, 124.02, 122.91, 118.55, 113.34, 108.29, 105.75, 97.87, 65.19, 51.70, 47.41, 44.54, 40.12, 12.78; Anal. calcd for C₃₆H₄₂N₆O₂: C, 73.19, H, 7.17, N, 14.23 %; found: C, 72.83, H, 7.63, N 13.76%.

Surface modification of silica gel with probe 2 (SiR-1)

2.5 g of silica gel(SiG) was stirred into 30 mL of an aqueous solution containing 10 % (v/v) 3-aminopropyl-triethoxy silane (APTES) at 50° C for 1 h. After silanization, the APTES modified silica gel was washed with deionized water several times to remove the residual silane. Then it was dried at 100 °C for 3h to allow cross linking of silanol groups to get APTES functionalized silica gel(SiA-1). Further, SiA-1 was taken in 100 mL of an aqueous solution containing 5% (w/w) glyoxal and allowed to react for 1h with constant stirring. The aldehyde incorporated surface modified silica gel was washed with excess deionized water and acetone sequentially to remove residual glyoxal. It was dried at 100 °C for 2h to get the yellow colored Schiff base product(SiA-2). A methanolic solution(10 mL) of **2** (0.254 g, 0.43 mmol) was added to methanolic suspension of the glyoxal appended yellow color silica particles (SiA-2, 2.0 g) priority added with few drops of glacial acetic acid, and heated to reflux for 7h with constant stirring. The residual product was filtered, washed with methanol and water repeatedly to remove the unreacted reactants and finally air dried to get the powdered like pale-yellow coloured probe immobilized silica particles SiR-1.

Results and Discussion

The probe **2** was synthesized through condensation of aminoethylrhodamine **1** with 2-amino pyridine-3-carboxaldehyde as per the synthetic route depicted in Scheme 1 and was characterized by ESI-MS, ¹H NMR and ¹³C NMR spectral analyses. The characteristic quaternary carbon peak near 65.19ppm in its ¹³C-NMR spectrum in CDCl₃ ascertained predominant existence of

rhodamine's spirolactam conformation. Similar to other known spirolactam derivatives^{12,16}, solutions of **2** in various organic solvents were also appeared colourless along with a weak fluorescence inferring to existence of spirolactam conformation. Its structure (Fig. 1), elucidated from X-ray diffracted data and analysis[‡] of its single crystals, has also confirmed spiro-cyclic rhodamine conformation in its architecture.

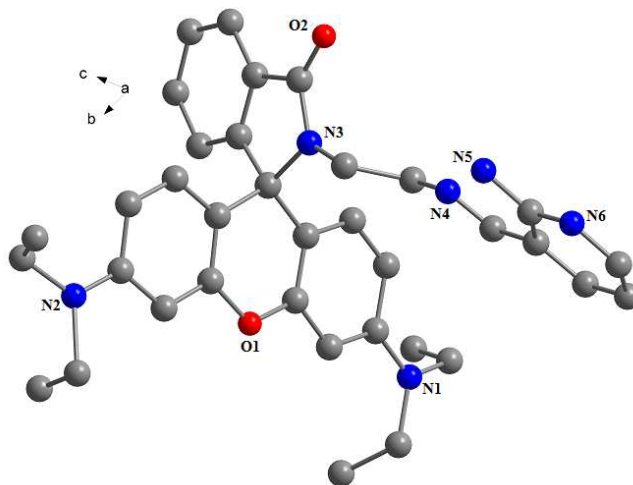


Fig. 1: Perspective view of crystal structure of **2** showing hetero-atom numbering scheme (H atoms are omitted for clarity).

Attachment of 2-amino-1-pyridyl moiety to the amino-end of receptor (N_4) has made a significant contribution to structural-electronic situation in the compound. Existence of a strong intra-molecular H-bonding between N_4 and N_5 ($N_4 \cdots N_5 = 2.773 \text{ \AA}$) was found in the asymmetric unit of **2** along with an intermolecular H-bonding ($N_5 \cdots N_6 = 3.001 \text{ \AA}$). The sum of angles around the amino-groups attached to xanthene core ($\Sigma \angle N_1 = 359.4^\circ$, $\Sigma \angle N_2 = 359.9^\circ$) inferred to a higher degree of pyramidalization over N_1 and N_2 , which also showed that the pyramidal geometries over N_1 and N_2 have not significantly deviated from their normalcy. The C–N bond length of amino groups attached to xanthene core were observed to be shorter (1.382–1.384 \AA) than the average C–N bond ($C_{30}-N_4 = 1.445 \text{ \AA}$). This is due to delocalization of electron density from N_1 and N_2 to aromatic- π - systems in the xanthene ring, inducing a partial double bond character of these N–C bonds. The angles around quaternary C_9 were observed to be 110.85° ($\angle C_{10}-C_9-C_{14}$), 112.26° ($\angle C_{12}-C_9-N_3$), 99.95° ($\angle C_{14}-C_9-N_3$) and 110.60° ($\angle C_{12}-C_9-C_{10}$) respectively, which indicated a slight deviation to its tetrahedral geometry due to amino-substitution at spiro ring. The torsion angles

between xanthene core (Xan) and its phenyl ring (Ph) were observed ($\angle O_1-C_9-C_{14}-C_{17}$) to be 150.75° while that between xanthene and pyridyl ($C_{34}-C_{32}-C_9-O_1$) was found to be 100.70° . The torsion angle between phenyl and pyridyl ($C_{34}-C_{32}-C_{19}-C_{16} = -166.98^\circ$) revealed that both of them are aligned in an out of plane manner in the molecule. The torsion angles between these spatially arranged donor atoms in the receptor moiety ($O_2-N_3-N_4-N_5$) was observed to be 55.72° . The non bonded distances among spatially disposed donor atoms (N_3, N_4, N_5 and O_2) along with the torsion angle among them represents a suitable cavity for effective metal-ion coordination.

Absorbance and fluorescence spectral responses of **2** in presence of metal ions

The colorless solution of probe **2** did not show any apparent absorption above 500 nm in MeCN or in MeCN-H₂O (1:1 v/v, PBS, pH 7.2) solution (conc. 1×10^{-5} M) due to its existence in spiroactam conformation of rhodamine. It has also exhibited a weak fluorescence ($\phi_{FT} < 0.001$), attributed to spirocyclic conformation that facilitates various non-radiative pathways to quench its fluorescence, apart from an operative photo-induced electron transfer processes from distal Amino-donor groups present in its receptor moiety.

In order to investigate the metal ion induced signaling pattern of **2**, perchlorate salts of various metal ions such as Na(I), K(I), Mn(II), Fe(II), Fe(III), Co(II), Ni(II), Cu(II), Zn(II), Pb(II), Ag(I), Cd(II) and Hg(II) were added to its solution in either MeCN or MeCN-H₂O (1:1 v/v) mixture. The choice of a mixed organic-aqueous medium primarily based on the solubility reason. Further, we have earlier reported^{12a,c} that presence of water molecules in an acetonitrile medium promote preferential Hg(II) coordination to ring-opened rhodamine in substituted ‘amino-ethyl-rhodamine’ based probes, where coordination of other metal ions to the probe gets restricted through their preferences of hydration over complexation to the probes. The colourless solution of **2** neither showed any enhancement in absorption nor emission intensities ($\lambda_{ex}=500\text{nm}$) on addition of Li(I), Na(I), K(I), Ca(II), Ba(II), Mn(II), Mg(II), Co(II), Ni(II), Zn(II), Cd(II) ions. On contrary, its colorless solution became pink upon addition of Hg(II) either in dry or aqueous acetonitrile medium showing a high absorption [$(\epsilon/\epsilon_0)_{\text{Hg(II)}}=196$ fold] at 557 nm due to metal ion induced spiro-ring opening (Fig. 2a). Although a little increase in absorption ($\epsilon/\epsilon_0 < 5$ fold) was observed on addition of Cr(III), Fe(II), Fe(III), Cu(II) and Pb(II) ions to its colorless solution, the metal ion induced absorption is apparently negligible in comparison to that upon addition of Hg(II) ion. Among all metal ions investigated apart from Hg(II) ion ($\epsilon_{2+\text{Hg(II)}}= 63253\text{dm}^3\text{mol}^{-1}$

$^1\text{cm}^{-1}$), **2** exhibited maximum enhancement in absorption with Fe(III) ion ($\epsilon_{2+\text{Fe(III)}} = 5979\text{dm}^3\text{mol}^{-1}\text{cm}^{-1}$). The chromogenic signal of **2** where its colorless solution turned into pink upon preferential complexation with Hg(II) could be detected through naked eye. Upon excitation at 500 nm, its quenched fluorescence enhanced ($\phi_{\text{FT}} = 0.672$) significantly with emission maxima at 580nm upon addition of Hg(II) ion (Fig. 2b). The enhanced fluorescence (I/I_0) of **2** upon addition of few other metal ions such as Cr(III), Fe(II), Fe(III), Cu(II) and Pb(II) was observed to be much less ($I/I_0 = 20\text{-}30$ fold) in comparison to that in presence of Hg(II) ion ($I/I_0 \sim 350$ fold). Therefore, its ‘turn-on’ signaling responses in MeCN-H₂O (1:1 v/v) that can be visually perceived as a function of colour change as well as instrumentally monitored through absorption and fluorescence enhancements, have rendered its high preferences towards Hg(II) ion among various metal ions under investigation.

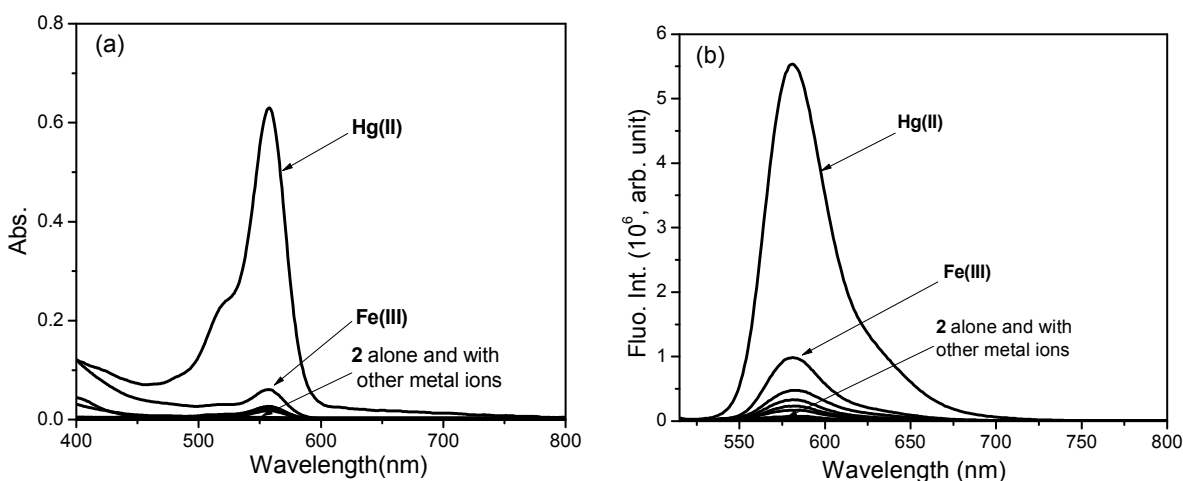


Fig. 2: Absorption (a) and fluorescence (b) spectra of **2** upon addition of various metal ions in MeCN-H₂O (1:1 v/v) medium. Absorption: $[\mathbf{2}] = 1 \times 10^{-5}\text{M}$, $[\text{M(I/II)}] = 2 \times 10^{-4}\text{M}$, Fluorescence: $[\mathbf{2}] = 1\mu\text{M}$, $[\text{M(I/II)}] = 25\mu\text{M}$, $\lambda_{\text{ex}} = 500$ nm, em. and ex. b. p. = 5nm, RT.

In a control experiment, the absorption and fluorescence spectral changes in **2** were monitored on sequential addition of Hg(II) ion (10 eq.) followed by other competitive metal ions (100 eq.) to that solution in MeCN-H₂O (1:1 v/v) in order to validate Hg(II) specific signaling responses of **2** and quantify the extent of possible interferences. Addition of these metal ions did not result in significant change to absorption and fluorescence intensities of the solution containing **2** with Hg(II) ion. On contrary, absorption (A_{557}) and fluorescence (I_{580}) was observed to increase significantly on addition of Hg(II) ion to the solutions containing **2** and each of these competitive metal ions (where $(\epsilon/\epsilon_0)_{557}$ or $(I/I_0)_{580}$ of $2 \ll \text{M(I/II)}$ either negligible or much lower). The

enhancements were up to a comparable extent of that of **2** in presence of Hg(II) ion alone. The comparative results thus obtained were indicative a remarkable high specificity of **2** for Hg(II) ion (Fig. 3a) in inducing photophysical signals of complexation mediated ring-opened rhodamine and standardized negligible interferences in signals due to other competitive metal ions coexisting in a sample.

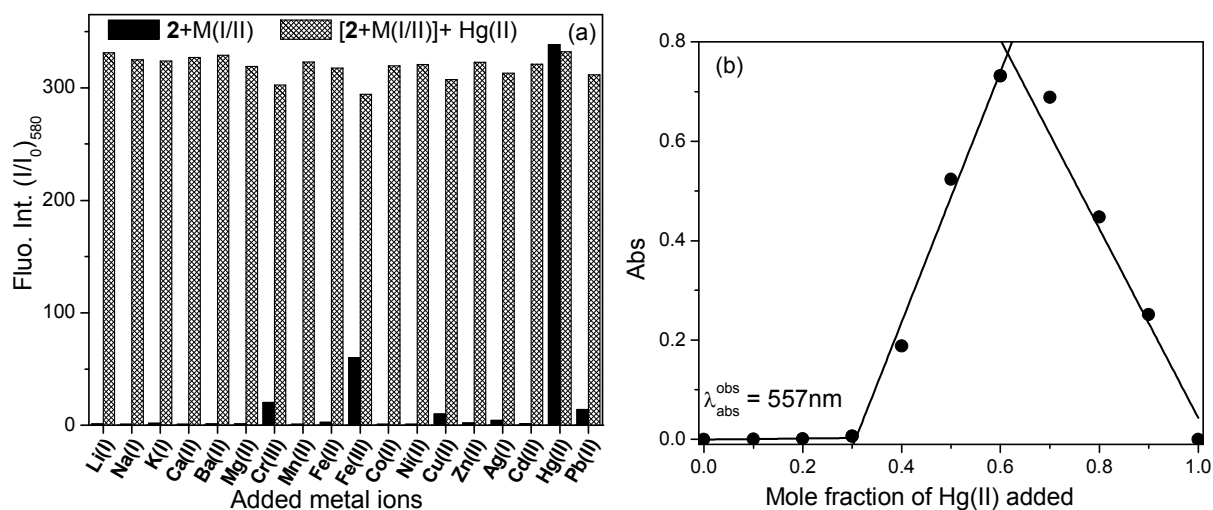


Fig. 3: (a) Fluorescence enhancement factors in **2** in presence of various metal ions followed by addition of Hg(II) ions in MeCN-H₂O(1:1 v/v) medium. [**2**] = 1 μM, [M(I/II)] = 25 μM, [Hg(II)] = 10 μM, $\lambda_{\text{ex}} = 500$ nm, em. and ex. b. p. = 5nm, RT. (b) Absorption of **2** as a function of mole fractions of added Hg(II) in MeCN-H₂O(1:1 v/v).

The compound showed slight increase in absorption and fluorescence upon addition of perchloric acid (H⁺ input), which is much lesser in comparison to that in presence of Hg(II) ion. Further, no appreciable enhancement in absorption (A_{557}) and fluorescence (I_{580} , $\phi_{\text{FT}} < 0.001$) spectral pattern of **2** was observed when measured in varied pH in 4.0-10.0 range. However, the spectral intensities were found to increase with decrease in pH values under more acidic conditions (pH < 4.0). The spectral responses of **2** in presence of Hg(II) in varying pH revealed that **2** yielded stable complexation mediated signal amplifications in 4.0-10.0 pH region without any interference by protons. Therefore, **2** and its Hg(II) complex was observed to be stable over a wide pH range for its potential utility in biological/complicated systems.

In order to verify whether anions of metal salt used impart any pronounced effect in the observed Hg(II)-ion induced absorption and fluorescence enhancements in **2**, HgCl₂ was used instead of Hg(ClO₄)₂ as ionic input under similar conditions which also resulted in a similar trend of

Hg(II)-induced absorption and emission signal amplification. On contrary, no such enhancements in intensities (A_{557} or I_{580}) in **2** were observed with $\text{Hg}(\text{OAc})_2$ as input, which inferred that Hg(II)-specific photophysical signaling behavior of **2** also depends upon counter anions present in medium.

The plot of absorption spectral responses of **2** monitoring at 557nm as a function of molar fraction of added Hg(II) ion in MeCN- H_2O (1:1 v/v) has determined the complexation stoichiometry of **2**-Hg(II) complex following continuous variation method (Job's Plot, Fig. 3b). The plot showed a maximum absorbance change near to 0.67 and an inflection point near to 0.5 mole fraction of Hg(II) added with **2**, supporting existence of 2:1 and 1:1 (**2**-Hg(II)) complexes respectively in the solution. In order to understand complexation pattern of **2** with Hg(II), absorption and fluorescence titrations were carried out in MeCN- H_2O (1:1 v/v) medium. Its UV-vis absorption (conc. = $1 \times 10^{-5}\text{M}$) spectral pattern as a function of added Hg(II) exhibited no appreciable change in absorption at 557nm upon addition up to 1.0 eq. of Hg(II), further gradual addition led to increase in A_{557} absorption transition with subsequent colourless \rightarrow pink colour transition till it attained maximum (up to 2.2 eq.) and remained constant there after even addition up to 10 eq. of Hg(II) (Fig. 4a). The absorption titration profile along with nature of Job's plot (Fig. 3b) suggested that the probe preferably coordinated first to one Hg(II) ion through donor atoms at distal 3-aminomethyl-(2-amino-1-pyridyl) receptor end resulting almost no increase in absorption, followed by coordination of other Hg(II) ion at amino ethyl-rhodamine in its ring opened form to exhibit enhanced absorption (A_{557}) and rendered the colour change. The fluorescence titration profile (Fig. 4b) of **2** (conc. = $0.2\mu\text{M}$) followed similar trend as that observed in absorption pattern. Its fluorescence intensity ($\lambda_{\text{ex}} = 500\text{nm}$) with emission maxima at 580nm exhibited enhancement to a smaller extent initially up to addition of 5eq. of Hg(II), enhanced significantly with gradual increase in Hg(II) concentration (up to 12 eq.) and remained constant thereafter saturation of complexation within a concentration threshold (even up to 50 eq.). Although **2** formed Hg(II) complex in a 1:2 (probe: metal ion) stoichiometry, absorption and fluorescence enhancements were appreciably observed only when the metal ion coordinated to aminoethyl-rhodamine in its ring-opened conformation, therefore, it is complicated to determine association constants for both metal ion complexation with the spectral profile of titration. The association constant (K_a) of **2**-Hg(II) complex was determined¹⁷ for a 1:1 (Probe:

metal ion) complexation stoichiometry assuming coordination of one Hg(II) ion that yielded the observed spectroscopic signals, was found to be $4.59 \times 10^7 \text{ M}^{-1}$ from the non-linear regression analysis of the fitting of fluorescence intensity of **2** as a function of Hg(II) concentration and comparable to those reported^{12a,b} for other Hg(II)-selective rhodamine based probes.

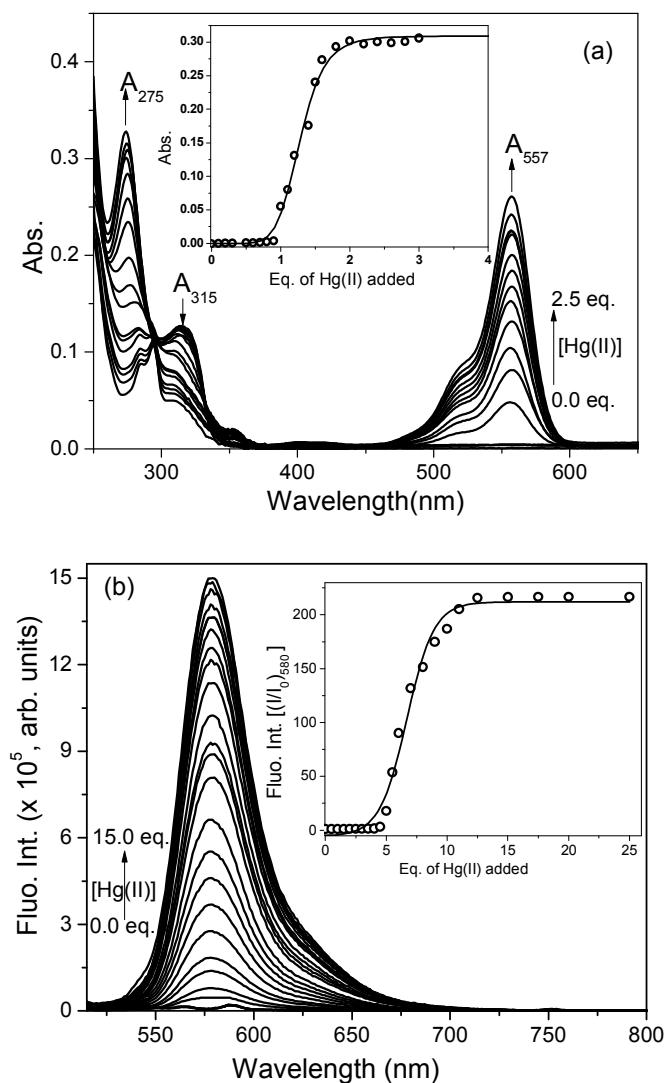


Fig. 4: (a) Absorption and (b) fluorescence spectral pattern as a function of added Hg(II) ion concentration. Abs: [**2**] = $1 \times 10^{-5} \text{ M}$, Em: [**2**] = $0.2 \mu\text{M}$, $\lambda_{\text{ex}} = 500 \text{ nm}$, RT, ex. & em. b. p. = 5 nm . Insets: (a) Abs. and (b) fluo. intensity profile of **2** versus eq. of Hg(II) added.

The detection limit (LOD) of Hg(II) binding to **2** was calculated¹⁸ as $3\sigma/s$ from the plot of change in fluorescence (I/I_0) as a function of concentration of Hg(II) added in a linear range, where σ is standard deviation of y-intercept and s is slope of linear regression of the graph. Based on fluorescence signal modulation, the detection limit was estimated to be $1.1 \times 10^{-8} \text{ M}$.

However, Hg(II) detection limit of **2** towards Hg(II) as a function of colour change observable through naked eye was found to be 5.0×10^{-6} M.

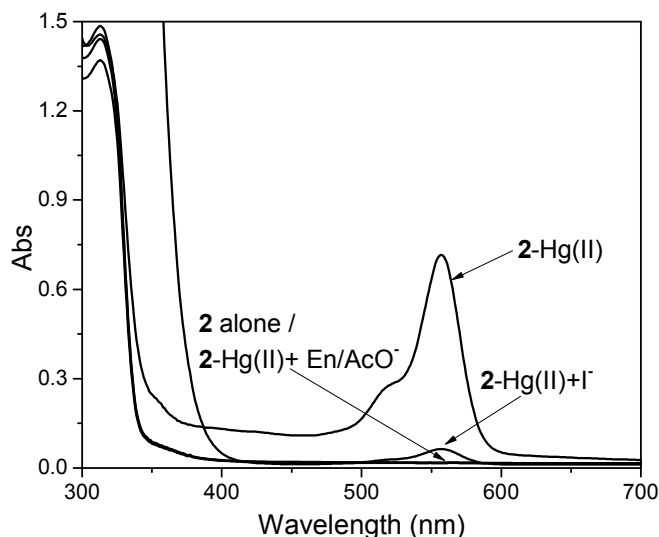


Fig. 5: Absorption spectra of *in-situ* **2**-Hg(II) complex in presence of I⁻(KI), AcO⁻ and ethylenediamine(En). [**2**] = 1×10^{-5} M, [Hg(II)] = 1×10^{-4} M, MeCN: H₂O (1:1 v/v).

A pre-requisite measure for any molecular ensemble to be chemosensor is its ability to exhibit reversibility in its signaling behavior, which in turn, promotes its reusability in detection of a particular analyte. In order to evaluate reversibility in signaling pattern of **2**, ammonium salts of various anions, complex reagents such as ethylenediamine (En), ethylenediamine tetra-acetic acid (EDTA) as well as various amino-acids were added to its solution containing Hg(II) in MeCN-H₂O(1:1 v/v) medium. The Hg(II)-induced spectroscopic output (A_{557} and I_{580}) of ring-opened rhodamine in **2** reverted back to that of uncomplexed **2** and pink colour of solution changed colourless again upon subsequent addition of few of those counter entities. Among all counter anions investigated, acetate (AcO⁻) anion resulted in almost quenching of Hg(II)-complexation mediated enhanced spectral features. Further, absorption and fluorescence spectral pattern of *in-situ* **2**-Hg(II) complex in presence of various amino acids revealed to a considerable decrease in spectral intensities on addition of few amino-acids such as L-proline, tryptophan, lysine, iso-leucine etc. and pink colour of the solution also turned almost colourless, the extent although not up to that of guest-free **2**. This inferred that Hg(II) ion in the probe-metal complex preferred to dislocate in favour of formation of a stronger complex of Hg(II) with these amino acids, while others amino-acids failed to induced any such change. Following displacement approach¹⁹, it is worth mentioning that the **2**-Hg(II) complex effectively discriminated²⁰ L-

proline(L-pro) in presence of its hydroxyl derivative *i. e.* 4-hydroxy proline (Hyp), which find a greater prospective as analytical methods in various biological and industrial applications. These observations inferred that any such entity having a higher binding affinity towards Hg (II) than the probe itself is capable in initiating de-complexation of **2**-Hg(II) complex, leading to its “Off-On-Off” signaling behavior. Moreover, subsequent addition of Hg(II) to the colourless solution of anion-mediated Hg(II)-decomplexed **2** ($\phi_{FT} < 0.001$) further resulted in spectral enhancements (A_{557} and I_{580}) almost to an extent of that upon initial Hg(II) addition to **2** ($\phi_{FT} = 0.654$) along with reappearance of pink colour of the solution, establishing the probe’s reusability in detection and estimation of Hg(II) concentration.

Immobilization of **2** onto silica gel surface

The metal ion induced spectral behavior of **2** therefore has endorsed its apparent potentiality in specific detection of Hg(II) ion at a low concentration level. It is imperative to investigate its optical signaling behavior upon its immobilization on to a solid surface such as silica gel for its practical utility in detection of Hg(II) ion. The immobilization process was carried out as per graphical representation depicted in Scheme 1 and characterized accordingly. Surface modification to silica gel (**SiG**) were done with immobilization of APTES on to its surface to yield **SiA-1**, which was further treated with glyoxal to result in a Schiff base product (**SiA-2**) at organic segment of the organic-inorganic hybrid (**SiA-1**). Finally, the desired probe appended surface modified silica based product(**SiR-1**) was obtained through Schiff-base condensation of **SiA-2** with **2**.

Characterization of **SiR-1**

The attachment of probe **2** onto the silica gel surface was confirmed from FTIR spectral pattern, thermogravimetric analysis, FESEM images and elemental analysis of **SiR-1** with respect to silica gel (**SiG**), **SiA-1** and **SiA-2**. The FTIR spectra revealed that silanol peaks (3713cm^{-1} , (Si)O-H str.) and 915cm^{-1} , (Si)O-H bend.) vanished upon surface modification of **SiG** with APTES, instead, appearance of new peaks corresponding to $-\text{CH}_2(2930\text{cm}^{-1}$, C-H str.) and $-\text{NH}_2$ (3460cm^{-1} , N-H str.; 1263cm^{-1} , C-N str.; 815cm^{-1} , N-H wag.) groups in that of **SiA-1** confirmed condensation of silanols with alkoxysilanes. Comparing with FTIR spectra of these compounds (**SiG**, **SiA-1** and **SiA-2**), appearance of few new peaks in **SiR-1** around 3050, 2170, 1805, 1630,

1530, 1245, 1090, 960, 750 (cm^{-1}) confirmed the attachment of organic layer containing probe **2** on to silica surface. The peaks corresponding to spiro lactam ring were not prominently observed, which might have shadowed under the peaks corresponding to substituted benzene rings. The sharp peak at 1266 cm^{-1} arising from C-N (str.) absorption corresponds to amino group attached in **SiR-1**. The absorption peak at $\sim 1030 \text{ cm}^{-1}$ corresponding to Si-O-Si str. frequency did not vary appreciably, which indicated that the primary structure of **SiG** did not change after silanization at its surface and subsequent attachment of probe **2**.

Thermogravimetric analysis (Fig. 6) of **SiR-1** in comparison to **SiG** revealed to a sharp fall in weight percentage attributed to loss of organic layer that contained probe **2**. The samples were heated from room temperature to $1000 \text{ }^\circ\text{C}$ in the typical TGA experimental conditions. In agreement with earlier reports²¹, **SiG** lost moisture at $120 \text{ }^\circ\text{C}$ with a weight loss of 3.48% and dehydroxylated in a single step process in $120\text{-}1000 \text{ }^\circ\text{C}$ range. On contrary, the surface modified **SiG** appended with APTES, i. e. **SiA-1** started losing organic component (APTES) after initial 1.03 % weight loss $120 \text{ }^\circ\text{C}$ in couple of steps. A 7.13% weight loss was observed in $120\text{-}550 \text{ }^\circ\text{C}$ range due to loss of APTES (boiling point of APTES is $217 \text{ }^\circ\text{C}$) followed by a 3.97 % weight loss in between $550 \text{ }^\circ\text{C}$ and $615 \text{ }^\circ\text{C}$ associated with loss of intraglobular hydroxyl groups. Similar degradation pattern was observed with **SiR-1** which underwent 1.48% initial weight loss in form of moisture at $120 \text{ }^\circ\text{C}$. Its thermogram exhibited 8.71% weight loss between $120 \text{ }^\circ\text{C}$ and $520 \text{ }^\circ\text{C}$, followed by a 5.32% weight loss between $520 \text{ }^\circ\text{C}$ and $615 \text{ }^\circ\text{C}$. In all cases, weight loss beyond $615 \text{ }^\circ\text{C}$ assumed to be due to dehydroxylation. Nevertheless, the complete organic segment in **SiR-1** was decomposed amounting to a 17.95% weight loss in comparison to **SiG**, comparable to those of other^{10c,11} mesoporous silica immobilized with rhodamine group. From the weight loss curves, the amount of **2** grafted in **SiR** was estimated to be 0.13 mmol/g .

In order to investigate the morphological changes on silica gel surface after immobilization of **2**, FESEM images (Fig.7) were taken for **SiG** and the probe (**2**) appended **SiR-1** surfaces. In comparison to smooth surface of **SiG**, rougher surface of **SiR-1** established immobilization of organic component onto its surface. The irregular particle size of **SiG** having average diameter $100 \text{ }\mu\text{m}$ was observed to be reduced upon immobilization, in turn, increased the surface area. In this context, the particle size distribution pattern of **SiR-1** dispersed in water medium suggested that its mean particle size is $56 \text{ }\mu\text{m}$ while the probe **2** agglomerated to form particles of 15 nm average size.

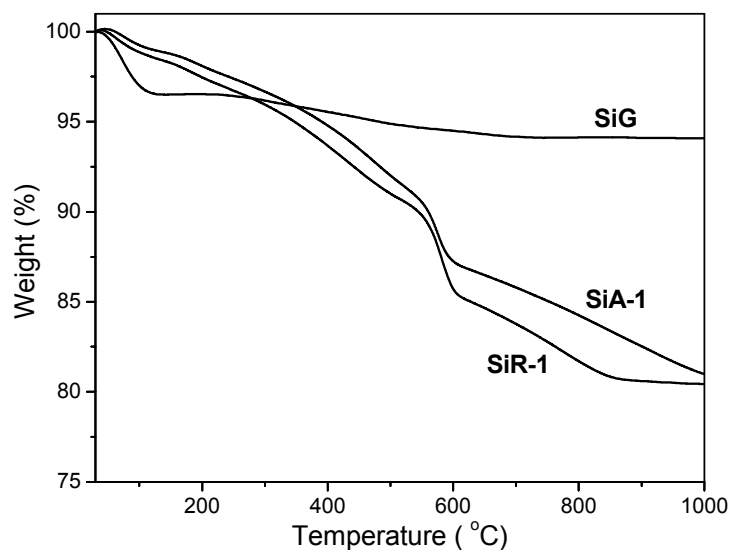


Fig. 6: Thermogravimetric plot of SiG, SiA-2 and SiR-1.

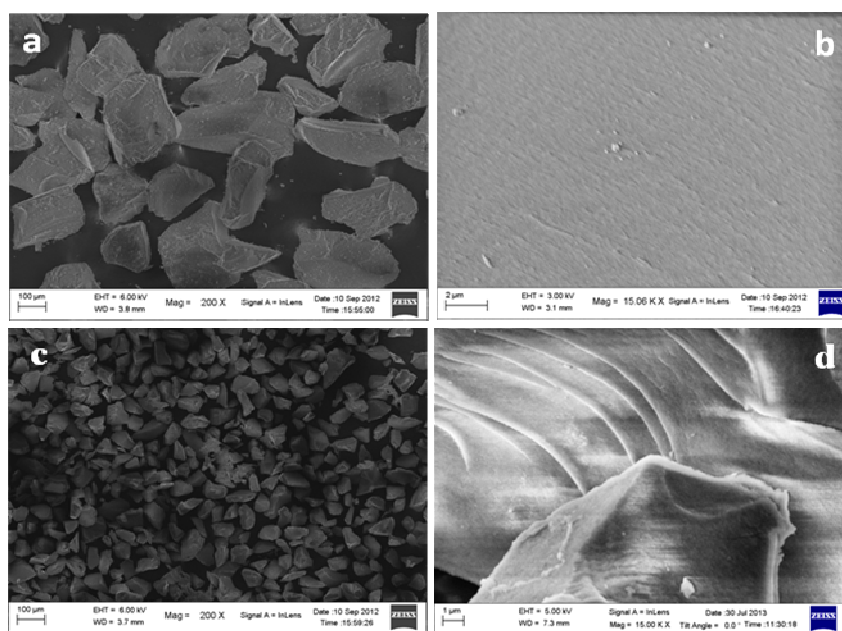


Fig. 7: FESEM images of SiG (a) and its surface morphology (b); the same after immobilization of **2** onto its surface (SiR-1) (c) and corresponding surface morphology(d).

The Hg(II) complex of SiR-1 was synthesized by adding SiR-1(0.01g) to an aqueous solution (3 mL) of 1 mM Hg(II), shaken mechanically at room temperature for 30 min. and centrifuged for 10 min at 5000 rpm. The supernatant was filtered-off and measured for unextracted Hg(II) ion by atomic absorption spectrophotometer. The analysis indicated that SiR-1 potentially adsorbed

86% of Hg(II) ion. The residual fraction was dried under vacuum to obtain the desired (SiR-1)-Hg(II) complex as reddish powder. The FTIR spectrum revealed that carbonyl (C=O) stretching frequency at 1630 cm^{-1} corresponding to spiro lactam ring of attached **2** in SiR-1 shifted to 1697 cm^{-1} in (SiR-1)-Hg(II) complex. Further, presences of Hg(II) ions in energy dispersive elemental spectra of (SiR-1)-Hg(II) complex also support the preferential coordination of Hg(II) to SiR-1. The comparative X-Ray diffraction pattern of SiG, SiR-1 and (SiR-1)-Hg(II) complex revealed that neither surface modification with organic content nor Hg(II) coordination to that organic content has altered the amorphous nature of silica gel. The intensity of broad reflection peak of SiG at 10.3° (2θ) remained almost same in SiR-1, however, decreased in case of (SiR-1)-Hg(II) complex.

The volume weighted particle size distribution pattern revealed that average size of particles of SiR-1 ($d_{0.5} = 56.96\mu\text{m}$, volume weighted mean $D[4,3] = 60.85\mu\text{m}$) decreases when the attached **2** in SiR-1 coordinates to Hg(II) ion ($d_{0.5} = 44.71\mu\text{m}$, volume weighted mean $D[4,3] = 55.50\mu\text{m}$). The Brunauer-Emmet-Teller (BET) surface area of SiR-1 and its Hg(II)-complex were calculated through nitrogen adsorption method in order to investigate the effect of complexation on its surface area. From the linearity of the plot at low relative pressure (p/p_0) of mesoporous materials, the BET surface area of SiR-1 was estimated to be $367.303\text{ m}^2/\text{g}$ which decreased to $182.669\text{ m}^2/\text{g}$ in (SiR-1)-Hg(II) complex. The lowered surface area of Hg(II)-complexed **2** in SiR-1 when compared to the un-complexed one indicative of a lower surface loading capability in former than later.

UV-vis absorption and fluorescence spectral behavior of SiR-1 with metal ions

The absorption spectral pattern of SiR-1 dispersed in an aqueous medium before and after addition of various metal ions such as Li(I), Na(I), K(I), Ca(II), Ba(II), Mg(II), Mn(II), Fe(II), Fe(III), Co(II), Ni(II), Cu(II), Zn(II), Cd(II) and Hg(II) are shown in Fig. 8a. An absorption peak in 500-600nm region (non-existent in of SiR-1) with absorption maximum at 561nm was observed to appear only in case of Hg(II) addition, indicating the Hg(II) complexation induced spiro lactam ring opening of **2** present in organic component attached to SiR-1 surface. Few other metal ions such as Fe(II), Fe(III) and Pb(II) also induced appearance of such peaks, but to a lesser extent in comparison to that with Hg(II) ion. The colour of the aqueous suspension of SiR-1 also changed from yellow to pink on addition of Hg(II). No such colour change observed on

addition of other metal ions. The fluorescence spectral responses (Fig. 8b) of **SiR-1** upon excitation at 400nm showed a fluorescence with maxima at 480nm, which may be attributed to the π -electronic interactions of the conjugated linker. The solution also showed very weak fluorescence intensity at 590nm. Upon addition of Hg(II), fluorescence intensity at 590nm enhanced inferring its ring-opened rhodamine induced by Hg(II)-complexation along with decrease in its fluorescence at 480nm. Such complexation induced fluorescence enhancements (I_{590}) were observed also with few other metal ions such as Fe(II), Fe(III) and Pb(II), however, to a much lesser extent in comparison to that with Hg(II). Other metal ions imparted either no or negligible change in its intensity at 590 nm. The probe **2** therefore retained its specificity towards Hg(II) ion when immobilized on to silica gel surface, inferring potentiality of **SiR-1** as a chemosensor for selective Hg(II) detection and isolation in presence of other interfering metal ions.

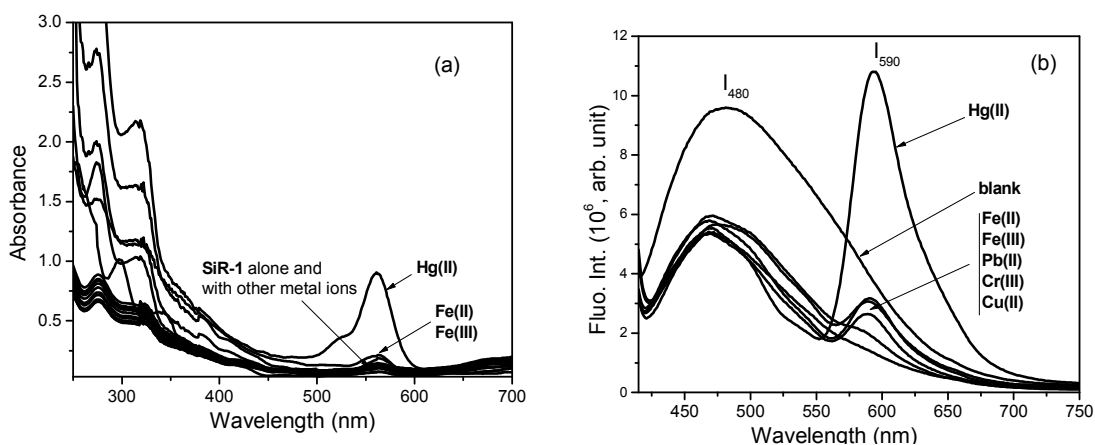


Fig. 8: (a) Absorption and (b) fluorescence spectra ($\lambda_{\text{ex}} = 400$ nm) of **SiR-1** upon addition of perchlorate salts of various metal in aqueous medium, $\lambda_{\text{ex}} = 400$ nm, em. and ex. b. p. = 5nm, RT.

The fluorescence peak with emission maxima at 480nm was observed (Fig. 9) to decrease and that at 590nm increase gradually with an isoemissive point at 568nm upon increase in Hg(II) ion concentration added to the suspension of **SiR-1** in aqueous-organic medium. Simultaneously, the colour of suspension deepens till it attained a reddish texture. The plot of ratiometric fluorescence output (I_{590}/I_{480}) as a function of molar concentration of added Hg(II) followed a sigmoidal pattern. In this context, a ratiometric mode is advantageous in terms of accuracy in detection than that with two discrete fluorescence signals. However, a detailed investigation with excited state lifetime measurements is required to understand the nature of fluorescence at

480nm (I_{480}) of **SiR-1** and its quenching in presence of various metal ions. Nevertheless, signaling responses of **SiR-1** in presence of Hg(II) is comparable with those of other^{10,11} surface modified silica appended with rhodamine reported in literature.

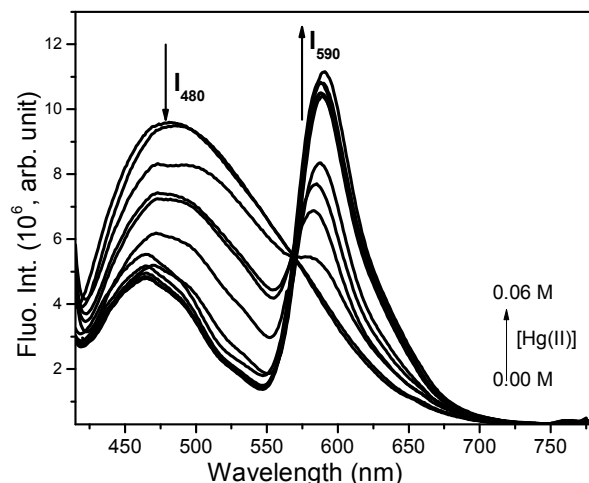


Fig. 9: Fluorescence spectral pattern of **SiR-1** upon addition of various concentration of Hg(II) in aqueous suspension. $\lambda_{\text{ex}} = 400 \text{ nm}$, em. and ex. b. p. = 5nm, RT.

As mentioned earlier, reversibility in signaling is a crucial parameter factors for a chemosensor for its practical application. The enhancement in absorption(A_{560}) and fluorescence(I_{590}) signals of **SiR-1** upon complexation with Hg(II) ion were reduced(Fig. 10) to an extent comparable that of uncomplexed **SiR-1** and an colour change from reddish to deep yellow(Fig. 11) was observed when counter anions like $\Gamma(\text{KI})$ and $\text{AcO}^- (\text{NH}_4\text{OAc})$ were added to suspension of (**SiR-1**)-Hg(II) complex in aqueous medium and mechanically shaken for 30 min.

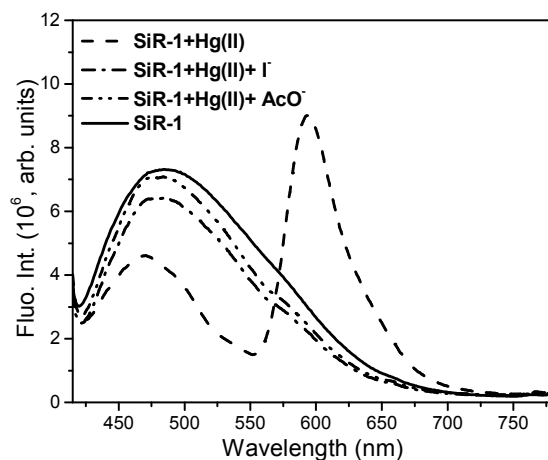


Fig. 10: Fluorescence spectra of (**SiR-1**)-Hg(II) upon addition of counter anions such as I- (KI) and OAc- (NH_4OAc) in aqueous medium, $\lambda_{\text{ex}} = 500 \text{ nm}$, em. and ex. b. p. = 5nm, RT.

The reversibility in absorption and fluorescence spectral pattern along with colour transition in SiR-1 establishes its repetitive usage in Hg(II) ion detection.



Fig. 11: Photographs of surface modified silica gel **SiR-1**, (**SiR-1**)-Hg(II), (**SiR-1**)-Hg(II) + KI (from left to right).

In order to establish potentiality of **SiR-1** in removal of Hg(II) ions from a solution containing various competitive metal ions, a controlled experiment was carried out by packing **SiR-1** particles in a column (6 cm × 1 cm dia.) where a synthetic solution containing Hg(II) and other interfering metal ions (conc. = 50 μM each) in aqueous medium was eluted. The atomic absorption spectral analysis of eluted solution revealed that Hg(II) ions were adsorbed by **SiR-1** inside the fabricated column by forming complexes with **SiR-1** while loss of molar concentration of interfering metal ions were restricted to <10%. Although other real-time parameters are to be manifested before developing a process for removal of Hg(II) ions with **SiR-1**, this experiment nevertheless demonstrates that this probe (**2**) when immobilized on a silica surface is also capable enough to detect and separate Hg(II) ion from other interfering metal ions.

Conclusion

The 3-aminomethyl-(2-amino-1-pyridyl)methyl derivatized amino-ethyl-rhodamine-B based probe **2** exhibited Hg(II)-specific chromogenic and fluorogenic signaling responses selectively among all metal ions investigated, where Its complexation induced structural transformation of attached rhodamine subunit with Hg(II) ion rendered a colorless→pink colour transition observable through naked eye(colour change) with a detection limit of 0.5×10^{-6} M and spectral perturbations as a function of absorption and fluorescence change with instrumentally manifested detection limit of 1.1×10^{-8} M. Its absorption and emission spectral enhancements in presence of Hg(II) ion reversibly reset in presence of counter anions rendering an “Off-On-Off” signaling module. Its Hg(II)-specific dual mode signaling pattern is also retained on its immobilization

onto a silica gel surface modified with a hydrocarbon chain that facilitate its attachment at its 'amino-ethyl-amino' receptor end. Although grafting of a rhodamine-G-hydrazide onto silica surface through a longer chain linker did not exhibit¹¹ any photophysical signaling responses with any metal ion, immobilization of the prefabricated Hg(II)-specific probe **2** onto silica gel (**SiR-1**) here exhibited Hg(II)-specific signal modulation in aqueous medium due to availability and appropriate spatial disposition of accessible donor sites for effective coordination. Further, probe **2** that exhibited Hg(II)-specific signal modulation in an organic-aqueous medium due to solubility issues, could effectively detect Hg(II) in aqueous medium when coupled to silica gel matrix, enhancing its potentiality in practical utilization. The adsorption ability of **SiR-1** was found to be 86% for Hg(II) ion. The surface modified silica-based probe was also demonstrated for efficient removal of Hg(II) ion from a mixture of competitive and interfering metal ions. Adopting similar methodology involving immobilization of prefabricated organic modules selective towards various metal ions onto solid matrix, development of probes is therefore anticipated to enhance the scopes for fabrication of tool-kit for spot monitoring of various metal ions and their subsequent removal in environmental prospective.

Acknowledgements

BPB wishes to thank DST, New Delhi for financial support (SB/EMEQ-226/2013) for this work and to the Director, CSIR-IMMT for infrastructural support.

Notes and references

‡ Crystal data for **2**: C₃₆H₄₂N₆O₂; M_w = 590.76; block-shaped; pale-yellow colour, triclinic, space group P $\bar{1}$, $a = 11.303(1)$ Å, $b = 11.742(1)$ Å, $c = 12.966(1)$ Å, $\alpha = 67.77(1)$, $\beta = 89.19(1)$, $\gamma = 86.47(2)$, $U = 1589.9(7)$ Å³, $T = 296(2)$ K, $Z = 2$, $\mu(\text{Mo K}\alpha) = 0.078$ mm⁻¹, $F(000) = 632$, $\rho_{\text{calc}} = 1.234$ mg/m³, 5401 reflection data with 402 parameters, 3753 [$I \geq 2 \sigma(I)$] unique reflections used in calculations. The final $R_1 = 0.0633$, $wR_2 = 0.1751$, $S = 1.021$. (CCDC No. 855628).

1. (a) *Heavy Metals in the Environment*. B. Sarkar (ed.), Marcel Dekker Inc., New York, 2002; (b) D. Beyersmann, in *Metals and Their Compounds in the Environment*, E. Merian (ed.); Wiley-VCH: Weinheim, 1990.

2. (a) D. Galaris, V. Skiada and A. Barbouti, *Cancer Lett.*, 2008, **266**, 21; (b) M. A. Lynes, Y. J. Kang, S. L. Sensi, G. A. Pedrizet and L. E. Hightower, *Ann. N. Y. Acad. Sci.*, 2007, **1113**, 159; (c) P. James and K. Raoul, *Analyst*, 2005, **130**, 528; (d) *Clinical Environmental Health and Toxic Exposure*. J. B. Sullivan and G. R. Kriger (eds.), 2nd edn., Lippincott Williams and Wilkins, Philadelphia, 2001; (e) J. J. R. F. D. Silva and R. P. J. Williams, *The Biological Chemistry of Elements: The Inorganic Chemistry of Life*. 2nd edn., Oxford University Press: Oxford, 2001; (f) J. B. Nielsands, *Biol. Met.*, 1991, **4**, 1.
3. (a) W. F. Fitzgerald, C. H. Lamborg and C. R. Hammerschmidt, *Chem. Rev.*, 2007, **107**, 641; (b) W. F. Fitzgerald, D. R. Engstrom, R. P. Mason and E. A. Nater, *Environ. Sci. Technol.*, 1998, **32**, 1; (c) A. Renzoni, F. Zino and E. Franchi, *Environ. Res.*, 1998, **77**, 68; (d) O. Malm, *Environ. Res.*, 1998, **77**, 73; (e) P. Grandjean, P. Weihe, R. F. White and F. Debes, *Environ. Res.*, 1998, **77**, 165; (f) T. W. Clarkson, *Crit. Rev. Clin. Lab. Sci.*, 1997, **34**, 369; (g) M. Harada, *Crit. Rev. Toxicol.*, 1995, **25**, 1.
4. (a) E. K. Silbergeld, I. A. Silva and J. F. Nyland, *Toxicol. Appl. Pharmacol.*, 2005, **207**, S282; (b) P. Kaur, M. Aschner and T. Syversen, *Neurotoxicol.*, 2006, **27**, 492; (c) E. R. Milaeva, *J. Inorg. Biochem.*, 2006, **100**, 905; (d) R. K. Zalups and S. Ahmad, *J. Am. Soc. Nephrol.*, 2004, **15**, 2023; (e) R. K. Zalups and L. H. Lash, *Toxicol. Appl. Pharmacol.*, 2006, **214**, 88; (f) G. Shanker, L. A. Mutkus, S. J. Walker and M. Aschner, *Mol. Brain Res.*, 2002, **106**, 1; (g) I. Oniyido, A. R. Norris and E. Buncel, *Chem. Rev.*, 2004, **104**, 5911; (h) H. H. Harris, I. J. Pickering and G. N. George, *Science*, 2003, **301**, 1203; (c) D. W. Boening, *Chemosphere*, 2000, **40**, 1335.
5. (a) M. Formica, V. Fusi, L. Giorgi and M. Micheloni, *Coord. Chem. Rev.*, 2012, **256**, 170; (b) N. Kaur and S. Kumar, *Tetrahedron*, 2011, **67**, 9233; (c) B. Bag and P. K. Bharadwaj, *Photo, Electrochemistry & Photobiology in the Environment, Energy and Fuel*, S. Kaneco ed., 2007, 201; (d) A. P. de Silva, B. McCaughan, B. O. F. McKinney and M. Querol, *Dalton Trans.*, 2003, 1902; (e) B. Valeur and I. Leray, *Coord. Chem. Rev.*, 2000, **205**, 3; (f) A. P. de Silva, D. B. Fox, A. J.M. Huxley and T. S. Moody, *Coord. Chem. Rev.*, 2000, **205**, 41; (g) K. Rurack, *Spectrochim. Acta A*, 2001, **57**, 2161; (h) A. P. de Silva, H. Q. N. Gunaratne, T. Gunnlaugsson, A. J. M. Huxley, C. P. McCoy, J. T. Radmacher and T. E. Rice, *Chem. Rev.*, 1997, **97**, 1515.

6. For selected reviews, see: (a) X. Li, X. Gao, W. Shi and H. Ma, *Chem. Rev.*, 2014, **114**, 590; (b) M. J. Culzoni, A. M. de la Pena, A. Machuca, H. C. Goicoechea and R. Babiano, *Anal. Methods*, 2013, **5**, 30; (c) X. Chen, T. Pradhan, F. Wang, J. S. Kim and J. Yoon, *Chem. Rev.*, 2012, **112**, 1910; (d) M. Beija, C. A. M. Afonso and J. M. G. Martinho, *Chem. Soc. Rev.*, 2009, **38**, 2410; (e) J. F. Jhang and J. S. Kim, *Anal. Sci.*, 2009, **25**, 1271; (f) H. N. Kim, M. H. Lee, H. J. Kim, J. S. Kim and J. Yoon, *Chem. Soc. Rev.*, 2008, **37**, 1465. Some recent examples for Hg²⁺ ion detection: (g) R. Bhowmick, R. Alam, T. Mistri, D. Bhattacharya, P. karmakar and M. Ali, *ACS Appl. Mater. Interfaces*, 2015, **7**, 7476; (h) C. Arivazhagan, R. Borthakur and S. Ghosh, *Organometallics*, 2015, **34**, 1147; (i) L. Li and Z. Fang, *Spectrosc. Lett.*, 2015, **48**, 578; (j) P. Xie, F. Guo, L. Wang, S. Yang, D. Yao and G. Yang, *J. Fluoresc.*, 2015, **25**, 319; (k) Z. H. Cheng, G. Li and M. M. Liu, *J. Hazard. Mater.*, 2015, **287**, 402; (l) Z. Sun, D. Guo, L. Zhang, H. Li, B. Yang and S. Yan, *J. Mater. Chem. B*, 2015, **3**, 3201; (m) J. Ni, B. Li, L. Zhang, H. Zhao and H. Jiang, *Sens. Actuat. B*, 2015, **215**, 174; (n) L. Feng, J. Sha, Y. He, S. Chen, B. Liu, H. Zhang and C. Lu, *Microporous Mesoporous Mater.*, 2015, **208**, 113; (o) L. Shen, Y. Wu and W. Ma, *Spectrochim. Acta A*, 2015, **138**, 348.
7. (a) Y. Q. Gao, J. Song, X. Zhao, S. Zhang, S. Xu, K. Wu and W. mou, *Sens. Actuat. B*, 2015, **215**, 292; (b) Z. H. Cheng, G. Li, N. Zhang and H. Liu, *Dalton Trans.*, 2014, **43**, 4762; (c) C. Kaewtong, B. Wannoo, Y. Uppa, N. Morakot, B. Pulpoka and T. Tuntulani, *Dalton Trans.*, 2011, **40**, 12578; (d) T. Balaji, S. A. El-Safty, H. Matsunaga, T. Hanaoka and F. Mizukami, *Angew. Chem. Int. Ed.*, 2006, **45**, 7202; (e) S. J. Lee, S. S. Lee, M. S. Lah, J.-M. Hong and J. H. Jung, *Chem. Commun.*, 2006, 4539; (f) U. Bach, D. Lupo, P. Comte, J. E. Moser, F. weissörtel, J. Salbeck, H. Spreitzer and M. Grätzel, *Nature*, 1998, **395**, 583; (g) L. Mercier and T. J. Pinnavaia, *Adv. Mater.*, 1997, **9**, 500.
8. (a) P. Yang, S. Gai and J. Lin, *Chem. Soc. Rev.*, 2012, **41**, 3679; (b) A. Schulza and C. McDonagh, *Soft Matter*, 2012, **8**, 2579; (c) Z. Jin, X.-B. Zhang, D.-X. Xie, Y.-J. Gong, J. Zhang, X. Chen, G.-L. Shen and R.-Q. Yu, *Anal. Chem.*, 2010, **82**, 6343; (d) W. S. Han, H. Y. Lee, S. H. Jung, S. J. Lee and J. H. Jung, *Chem. Soc. Rev.*, 2009, **38**, 1904; (e) M. Numata, C. Li, A.-H. Bae, K. Kaneko, K. Sakurai and S. Shinkai, *Chem. Commun.*, 2005, 4655; (f) L. Zhang, W. Zhang, J. Shi, Z. Hua, Y. Li and J. Yan, *Chem. Commun.*, 2003, 210.
9. (a) D. Lu, L. Yang, Z. Tian, L. Wang and J. Zhang, *RSC Adv.*, 2012, **2**, 2783; (b) H. J. Kim, S. J. Lee, S. Y. Park, J. H. Jung and J. S. Kim, *Adv. Mater.*, 2008, **20**, 3229; (c) K. Sarkar, K.

- Dhara, M. Nandi, P. Roy, A. Bhaumik and P. Banerjee, *Adv. Funct. Mater.*, 2009, **19**, 223;
- (d) Q. T. Meng, X. L. Zhang, C. He, G. J. he, P. Zhou and C. Y. Duan, *Adv. Funct. Mater.*, 2010, **20**, 1903.
10. (a) B. Liu, F. Zeng, G. Wu and S. Wu, *Chem. Commun.*, 2011, **47**, 8913; (b) Z. Dong, X. Tian, Y. Chen, J. Hou and J. Ma, *RSC Adv.*, 2013, **2**, 2227; (c) M. H. Lee, S. J. Lee, J. W. Jung, H. Lim and J. S. Kim, *Tetrahedron*, 2007, **63**, 12087.
11. W. Huang, D. Wu, G. Wu and Z. Wang, *Dalton Trans.*, 2012, **41**, 2620.
12. (a) B. Bag and A. Pal, *Org. Biomol. Chem.*, 2011, **9**, 4467; (b) B. Bag and B. Biswal, *Org. Biomol. Chem.*, 2012, **10**, 2733; (c) B. Biswal and B. Bag, *RSC Adv.*, 2014, **4**, 33062.
13. M. Fischer and J. Georges, *Chem. Phys. Lett.*, 1996, **260**, 115.
14. B. Bag, P. K. Bharadwaj, *J. Phys. Chem. B*, 2005, **109**, 4377.
15. (a) X. Zhang, Y. Shiraishi and T. Hirai, *Org. Lett.*, 2007, **9**, 5039; (b) H. Soh, K. M. K. Swamy, S. K. Kim, S. Kim, S. -H. Lee and J. Yoon, *Tetrahedron Lett.*, 2007, **48**, 5966.
16. Some recent examples: (a) L. Yao, B. Shen, C. Cao, W. Feng and F. Li, *RSC Adv.*, 2014, **4**, 20252; (b) N. R. Chereddy, S. Thennarasu and A. B. Mandal, *Analyst*, 2013, **138**, 1334; (c) Y.-S. Mi, Z. Cao, Y.-T. Chen, Q.-F. Xie, Y.-Y. Xu, Y.-F. Luo, J.-J. Shi and J.-N. Xiang, *Analyst*, 2013, **138**, 5274; (d) X. Chen, X. Meng, S. Wang, Y. Cai, Y. Wu, Y. Feng, M. Zhu and Q. Guo, *Dalton Trans.*, 2013, **42**, 14819; (e) W. Wang, Y. Li, M. Sun, C. Zhou, Y. Zhang, Y. Li and Q. Yang, *Chem. Commun.*, 2012, **48**, 6040; (f) K. Ghosh, T. Sarkar and A. Sammader, *Org. Biomol. Chem.*, 2012, **10**, 3236; (g) F. Wang, S.-W. Nam, Z. Guo, S. Park and J. Yoon, *Sens. Actuat. B*, 2012, **161**, 948; (h) S. Saha, P. Mahato, G. U. Reddy, E. Suresh, A. Chakrabarty, M. Baidya, S. K. Ghosh and A. Das, *Inorg. Chem.*, 2012, **51**, 336.
17. Q.-X. Liu, Z.-Q. Yao, X.-J. Zhao, Z.-X. Zhao and X.-G. Wang, *Organometallics*, 2013, **32**, 3493.
18. G. L. Long and J. D. Winefordner, *Anal. Chem.*, 1983, **55**, 712A.
19. (a) X. Lou, L. Zhang, J. Qin and Z. Li, *Langmuir*, 2010, **26**, 1566; (b) C. Luo, Q. Zhou, B. Zhang and X. Wang, *New J. Chem.*, 2011, **35**, 45; (c) Y.-B. Ruan, A. -F. Li, J.-S. Zhao, J. -S. Shen and Y.-B. Jiang, *Chem. Commun.*, 2010, **46**, 4938.
20. A. Pal and B. Bag, *RSC Adv.*, 2014, **4**, 10118.
21. (a) L. Saikia, D. Srinivas and P. Ratnaswamy, *Appl. Catal. A*, 2006, **309**, 144; (b) E. Satu, E. Root, M. Peussa and L. Niinisto, *Thermochem. Acta*, 2001, **379**, 201.